Long-term monitoring of surface reflectance, NDVI and clouds from space: What contribution we can expect due to effect of instrument spectral response variations?

Alexander P. Trishchenko[*a], Josef Cihlar[a], Zhanqing Li[b], Byongjun Hwang[c]
[a]Canada Centre for Remote Sensing, [b]University of Maryland, [c]Intermap Technologies Corp.

ABSTRACT

Since the satellites provide frequent and global observations of atmospheric and terrestrial environment, attempts have been made to use satellite data for long-term monitoring of land reflectances, vegetation indices and clouds properties. Although the construction and characteristics of spaceborne instruments may be quite similar, they are not identical among all missions, even for the same type of instrument like AVHRR. Consequently, the effect of varying spectral response may create an artificial noise imposed upon a subtle natural variability.

We report the results of a study on the sensitivity of Normalized Difference Vegetation Index (NDVI), surface and cloud reflectance to differences in instrument spectral response functions (SRF) for various satellite sensors. They include AVHRR radiometers onboard NOAA satellites NOAA-6 - NOAA-16, the Moderate Resolution Imaging Spectroradiometer (MODIS), the VEGETATION sensor (VGT) and the Global Imager (GLI). We also analyzed the SRF effects for several geostationary satellites used for cloud studies, such as GOES-8 – 12, METEOSAT-2 – 7, GMS –1 – 5. The results obtained here demonstrate that the effect of instrument spectral response function cannot be ignored in long-term monitoring studies that employ space observations from different sensors. The SRF effect introduces differences in observed reflectances and retrieved quantities that may be comparable or exceed the range of natural variability and possible systematic trends, the contribution from the calibration, atmospheric and other corrections. Some modeling results were validated against real satellite observations with good agreement.

Keywords: spectral response function, satellite observations, monitoring, surface reflectance, NDVI, clouds.

1. INTRODUCTION

Unique capability of spaceborne systems to provide global frequent observations combined with availability of quality satellite data records for more than two decades naturally leads to the idea of monitoring potential long-term changes in the Earth's environment from space. To achieve this goal, one needs to use observations with identical or very similar properties to ensure continuity of the data record between successive missions or systems. The surface air temperature measurements may serve as an example of traditional meteorological observations, even though the measurement properties of temperature sensors, like accuracy, inertia, stability etc. may differ between models. However, in any circumstances these sensors provide thermodynamic temperature of the air at the point of location, which is a well-defined property of the environment. For satellite remote sensing observations, the situation is more complicated. Most satellite observations are the measurements of electromagnetic radiation at the top-of-the-atmosphere (TOA) level within spectral bands located in the solar shortwave (SW) or thermal longwave (LW) part of spectrum. Therefore, these data need to be processed in a certain way to ensure that they correspond to a specific parameter characterizing the state of the environment: surface, atmosphere or clouds.

The processing of satellite data involves many steps. The final purpose of satellite data processing is to obtain the systematic maps of various quantitative physical parameters corrected for the intervening effect of atmosphere, varying observational geometry and specific sensor properties. Some of these corrections can be done quite accurately, like the correction for Rayleigh molecular scattering. Nonetheless, most of them may be implemented with some uncertainty due to limited knowledge of the input information.

The most important processing step is the data calibration. Despite numerous efforts, the results often vary among different investigators (Brest et al., 1997; Rao and Chen, 1999; Gutman, 1999; Masonis and Warren, 2001; Tahnk and Coakley, 2001). It is commonly agreed that for satellite sensors lacking onboard calibration in the solar spectrum, the

total relative uncertainties of calibration are within 5% (Rossow and Schiffer, 1999). An essential part of this uncertainty may be related to the effect of the spectral response function, when it is not accounted for properly during vicarious calibration or sensor intercalibration (Teillet et al., 2001).

Variable sun and observational geometry induces another source of systematic noise (Gutman et al., 1989). This angular effect is a combination of anisotropic reflective properties of the atmosphere and land surface. The effect must be accounted for in long-term studies of satellite data to obtain unbiased results (Cihlar et al., 1998; Gutman, 1999). This is achieved by normalizing satellite images to a common geometry using empirical anisotropic factors. They are derived either from a sequence of satellite scenes collected over long period of time (Cihlar et al., 1998, Trishchenko et al., 2001a) or from special directional observations like those ones from POLDER or MISR instruments (Csiszar et al., 2001).

Numerous vegetation indices have been developed to monitor the state of vegetation from spaceborne instruments. They were constructed to diminish atmospheric contamination, mitigate the influence of soil spectral reflectance signatures, or emphasize vegetation condition. The set of advanced vegetation indices optimised for up-coming sensors is discussed by Gobron et al. (2000). Nevertheless, NDVI remains the basic vegetation index most widely employed for global monitoring of vegetation. It is defined as the following ratio

$$NDVI = \frac{\rho^{NIR} - \rho^{red}}{\rho^{NIR} + \rho^{red}},$$ (1)

where ρ^{NIR} and ρ^{red} are reflectances for visible (red) and NIR spectral bands.

An important application of satellite observation is to retrieve cloud properties: cloud fraction, optical thickness, cloud type and other parameters (Rossow and Schiffer, 1999, Trishchenko et al., 2001b). This application employs quite a wide range of polar orbiting and geostationary sensors with very dissimilar properties. Even though the possible effect of varying SRF was noted as important for these studies (Desormeaux et al., 1993; Brest at al., 1997), so far it was not studied in a systematic way for long-term monitoring.

Attempts have been made to use the AVHRR data for long-term monitoring of land reflectances and vegetation indices (Gutman, 1999; Kaufman et al., 2000; Cihlar et al. 2002). These and other studies on long-term monitoring are motivated by the availability of quality AVHRR data for a period of nearly twenty years. Although the construction and characteristics of all AVHRR instruments are quite similar, they are not identical among all missions. Consequently, the effect of varying spectral response between sensors may create an artificial noise in the data time series imposed upon a subtle natural variability. This artifact should be examined thoroughly before comparing data between different missions to determine possible changes in satellite climatic records. So far, the effects of spectral response functions have not been considered carefully in such studies. Some aspects of the spectral characteristics of satellite sensors on remote sensing of vegetation indices have been studied for forested regions (Teillet et al., 1997) and in the context of vicarious calibrations procedures (Teillet et al., 2001). Nevertheless, systematic characterization of these effects for various representative surface spectral signatures on a global scale and for all AVHRR sensors has not been properly addressed. Analysis of long-term satellite products from various missions may require corrections to account for differences in SRF that have not been investigated.

Our study is aimed to fill this gap and to provide quantitative estimates for the effect of SRF among various satellite missions. Differences between AVHRR and MODIS, GLI and VEGETATION sensors are considered in land surface applications. To assess the impact of SRF effect in cloud studies, we conducted comparisons of modeling results between visible channels of AVHRRs and corresponding channels of geostationary satellites: GOES, METEOSAT and GMS.

2. THE EFFECT OF SPECTRAL RESPONSE FUNCTION

The spectral band average observed radiance and reflectance are obtained by convolution of spectral flux or radiance and instrument spectral response function $f(\lambda)$. For example, band average reflectance is given by

$$\overline{\rho} = \frac{\int_{\lambda\min}^{\lambda\max} L^{\uparrow}(\lambda)f(\lambda)d\lambda}{\int_{\lambda\min}^{\lambda\max} S^{\downarrow}(\lambda)f(\lambda)d\lambda} = \frac{\int_{\lambda\min}^{\lambda\max} S^{\uparrow}(\lambda)\rho(\lambda)f(\lambda)d\lambda}{\int_{\lambda\min}^{\lambda\max} S^{\downarrow}(\lambda)f(\lambda)d\lambda},$$ (2)

where $L^\uparrow(\lambda)$ and $S^\downarrow(\lambda)$ are spectral upwelling and downwelling radiation at the TOA or surface levels; $\rho(\lambda)$ is spectral reflectance of observed target (surface or cloud top), λ is a wavelength. Expression (2) shows that when spectral limits and shape of the spectral response function $f(\lambda)$ vary from sensor to sensor one cannot expect that corresponding band average quantities to be equal to each other unless spectral variations of the solar flux and target reflectance are negligible within band the limits.

Figure 1 shows some surface spectra of vegetated and non-vegetated targets (left panels) as well as spectral response functions of several coarse resolution sensors used for land studies (right panels). Noticeable differences are seen between the shapes of SRFs for various sensors and their location relative to the vegetation transition band around 0.7 μm. To encompass a potential range of variability in surface reflectance and NDVI, a set of representative spectra for various surface targets were compiled, following the classification scheme used in the NASA Surface and Atmospheric Radiation Budget (SARB) Project (Rutan and Charlock, 1997). The complete scheme for the SARB Project included 20 different surface classes. Since we had no measurements for some of the surface types, and the particular focus of this study was on the boreal ecosystem, 12 classes were adopted in this investigation as shown in Figure 1. Surface classes of lower class number nevertheless covered the bulk of variability in spectral reflectance that occurrs in nature. Classes 1 and 2 are depicted by two spectral curves each, and class 6 (grassland) is described by 4 curves with different values of NDVI to reflect various vegetation density levels.

Spectral curves were derived from two sources. The first source was aircraft observations from the PROBE-1 instrument made by the Canada Centre for Remote Sensing (Secker et al., 1999). The PROBE-1 is an airborne hyper-spectral sensor with 128 spectral bands covering the visible and near-infrared spectral regions. The second source was the ASTER (Advanced Spaceborne Thermal Emission and Reflection Radiometer) spectral library (available from http://speclib.jpl.nasa.gov). We normalized each spectrum to reproduce SARB broadband albedo. This normalization links individual spectral curves to a specific SARB surface type. The derived spectra (Figure 1, left) are shown for the wavelength interval 0.35-1.25 μm, which essentially covers the visible and NIR portion of the solar spectrum under study. The top panel depicts spectra of non-vegetated surfaces and a dry grass/savannah surface, and the bottom panel shows spectra for various vegetated surfaces. The steep increase in reflectivity above 0.7μm is a characteristic feature of these curves. The data selected encompass spectral differences between various natural surface classes.

Figure 2 shows the situation for the sensors used in cloud studies. Sensors under consideration include AVHRR/NOAA-9 to 16, visible channels of the imagers on GOES-8 to 12, METEOSAT –2 to 7, GMS-1 to 5. Spectral reflectance of middle clouds (*As)* with an optical depth of 20 and spectrum of solar extraterrestrial radiation are plotted for reference. Clearly, variability in scene spectral reflectance and solar spectral flux are not negligible within band spectral limits and, therefore, the SRF effect has to be taken into account to explain possible variations in observed cloud properties and reflectances between various sensors.

The 6S radiative transfer code (Vermote et al., 1997) was employed for clear-sky model simulations. Modtran 4.2 radiative transfer code with built-in and cloud models were used for modeling cloud scenes (Berk, Anderson, et al., 2001 and 1999). We considered 6 cloud models (St, Sc, Cu, Ns, As, Ci) with optical depth varied from 1 to 100. Cloud layers were assumed plane-parallel and were placed into different standard atmospheres with variable temperature profile, water vapor and ozone contents. The solar zenith angle varied from 5 to 80 degrees. The total number of simulated cloud spectra was ~3000.

3. RESULTS

3.1 Land surface

Figure 3 shows the surface level results for visible (red) and NIR reflectances. The absolute and relative differences with respect to AVHRR/NOAA-9 values are plotted against NDVI for each sensor. The least differences relative to AVHRR/NOAA-9 are found for AVHRR/NOAA-11 followed by NOAA-12. Other AVHRR/1,2 radiometers are reasonably close to AVHRR/NOAA-9, although the differences could reach 0.01 (10-15% relative) for the red channel and 0.01 (2-3%) for the NIR channel. Differences for NDVI at the surface and TOA levels are presented in Figure 4. Differences up to 0.03 (4-6%) for the NDVI of vegetated surfaces can be observed. Since NDVI for sparse vegetation and non-vegetated targets are small, the relative differences in NDVI for these surface types are larger.

The sensor spectral reflectances and NDVI differ systematically for AVHRR/3 onboard NOAA-15 and NOAA-16. The visible (red) reflectance for AVHRR/3 is smaller by 0.01-0.015 (20-25%), while the NIR channel reflectance is larger by 0.01-0.015 (3-4%). As a result, NDVI derived from AVHRR/NOAA-15 or -16 is higher by 0.03-0.06 (5-10%). These differences are due to (i) the significantly narrower spectral band of the visible (red) channel that is much less

contaminated by the elevated reflection in the NIR; (ii) the NIR channel that is is less influenced by the transition band (Figure 1).

The SRFs of MODIS and GLI are so different from that of AVHRR/NOAA-9 that the surface reflectance differences reach 0.02 (20-30%) in the visible channel, 0.04-0.05 (10-15%) in the NIR channel, and 0.06-0.09 (20-25%) for the NDVI. The SRF effect for VGT is smaller than for MODIS and GLI, and comparable to AVHRR/3. The difference could be as large as 0.01 (~10%) in the visible (red) channel, 0.02-0.04 (5-10%) in the NIR channel, and 0.03 (~5-10%) for the NDVI for vegetated surfaces. A method to correct for discrepancies caused by different SFRs is proposed by Trishchenko et al. (2002). It employs a second-degree polynomial fit as function of NDVI.

The general trends of the effect of varying SRF at the TOA are similar to those at the surface, but they do differ in detailed features as a result of the distortion by the atmosphere. Discrepancies in TOA simulated NDVI with respect to AVHRR/NOAA-9 are shown in Figure 4 (right panel). Quadratic fits to the relative differences in reflectances and absolute difference in NDVI are also plotted. Other data points are more scattered and no fits are presented. For example, the relative difference for NDVI may be extremely large for some combinations, simply because NDVI values computed at the TOA level are very close to zero. The right panel of Figure 4 contains more points than figures for the surface level because of the variable effects of the atmosphere and observation geometry. Therefore, fitting all data points with one curve is just a bulk approximation of the SRF effect to account for the large SRF effect (e.g., MODIS, VGT, GLI). In the case of AVHRR sensors, the approach still provides a good approximation of the effect of SRF. Similar to the surface case, the best agreement with AVHRR/NOAA-9 was found for AVHRR/NOAA-11. For all remaining AVHRRs, the atmospheric effect generally diminishes the spectral difference for the visible (red) channel and slightly increases it for the NIR channel. The absolute discrepancies in NDVI remain essentially the same as at the surface, 0.03-0.06. The effect on NDVI for NOAA-7, -8, -11, -12 and -14 is typically within ±0.01. For NOAA-6 and NOAA-10, the differences in NDVI relative to NOAA-9 were as much as 0.02-0.03 (3-5% for vegetated surfaces). The largest discrepancy was observed for NOAA-15 and -16. The absolute difference in NDVI could be as high as 0.03-0.06, which is larger than 10% for vegetated targets.

The corrections for the visible channels of MODIS, VGT and GLI sensors at the TOA are similar in magnitude to those at the surface, but the magnitude of spectral correction for the NIR channels is much higher (not shown). Apart from the same reasons as for the surface, the narrow NIR spectral channels are not affected by atmospheric absorption in the 0.94 µm water vapor absorption band. Consequently, the relative differences between these sensors and AVHRR/NOAA-9 were as much as 20-40%, with the largest differences occurring between AVHRR and MODIS (up to 40%). The results for VGT and GLI are similar but smaller than for MODIS. The difference ($\rho_{NIR} - \rho_{NIR,NOAA-9}$) is positive in all cases and increases with NDVI.

The comparison of modeling results to real satellite data is presented in Figure 5. The comparison is between clear-sky composites from MODIS and AVHRR/NOAA-14 over an area of Southern Great Plains (USA). The MODIS data cover the period from 19 July to 26 July, 2000 and the AVHRR data cover for the period from 21 July -31 July, 2000. All images were resampled to Lambert conformal conic projection with a 1 km resolution. The area of comparison is 10^Ox8^O centred around (36^ON; 97^OW). Joint statistical distributions of reflectances and brightness temperatures were analysed and additional thresholds were applied to all images to detect and to remove cloud-contaminated pixels, in addition to applying clear-sky compositing procedures. Water pixels were excluded from the comparison due to their strong directional effects that would complicate the comparison (Cihlar et al., 2001). The directional effects resulting from different local observation times and geometry do exist over land as well, but are less pronounced than over water. The effect is further reduced for NDVI due to considerable cancellation of the effects in the visible and NIR channels (Gutman, 1999). Statistical analysis using the t-test showed that the two comparisons have a statistically significant non-zero mean difference at a significance level of 0.01 or lower. The observed modal value of the NDVI difference is 0.14 (29%) and the mean difference is 0.15 (31%), in comparison with the modeled NDVI difference of about 0.125 (25%). Slightly smaller values of NDVI difference for the modeling case may reflect the contribution of water vapor effect (Trishchenko et al., 2002). Good overall agreement between modeling estimates and satellite observations bolsters our confidence in the estimates of spectral correction effects described above.

3.2 Cloud scenes
Figure 6 shows results for cloud scenes. As before, all comparison are made relative to the visible channel of AVHRR/NOAA-9, which is considered as the reference sensor (Rossow and Schiffer, 1999). Results are compared for the quantities at the TOA.

A comparison revealed that the differences in cloud reflectance among the AVHRR radiometers relative to AVHRR/NOAA-9 ranged mostly from -2% to +2% for visible channel (red) for most cases. The most significant difference was observed for the AVHRR/3 radiometers (NOAA-15 and –16) with the difference being be as high as –7% for optically thin clouds. Consistent results were obtained with the AVHRR sensors aboard NOAA-9, NOAA-11 and –12 satellites. The comparisons for the visible channel of geostationary imagers on GOES spacecrafts showed that corresponding differences are within 5% for optically thick clouds (reflectance ρ>0.4). For ρ < 0.2 (optically thin clouds), the differences vary from 2% to 35%. The largest deviations exist for GOES-11. For METEOSAT, the differences in general are largest among all missions . Biases are within 20% for optically thick clouds (ρ>0.4). For ρ < 0.2, differences vary from 20% to 80%. The largest deviations were observed for METEOSAT-2. These results are explained by very large differences in the spectral coverage and shape of the METEOSAT visible channel SRF relative to AVHRR/ NOAA-9 visible channel SRF. The SRFs cover range from 0.3 µm to more than 1 µm. As such, the METEOSAT band average reflectance is affected by variability in spectral reflected radiation within the METEOSAT spectral band, but also variability of surface spectral reflectance for optically thin clouds. Significant differences also exist for GMS imagers. They vary from 5 to 10% for optically thick clouds with reflectance ρ>0.4. For optically thin clouds (ρ < 0.2) the differences vary from 5% to 25-30%. They may be as high as 80% for GMS-5. The largest deviations were observed for GMS 5 due to wide SRF that covers the visible and the NIR spectral regions up to 1.1 µm.Results of the comparison as presented in Figure 6 show that the best way for consistent retrievals of cloud properties is to do it on a sensor-by-sensor basis. The unified retrieval technique applied for the TOA reflectances without distinction between satellite channels may lead to systematic biases in retrieved parameters.

CONCLUSIONS

Long-term monitoring of the Earth's environment by satellite sensors require consistent and comparable measurements. In this paper, we evaluated the effect of a major sensor parameter, namely the spectral response function, on the consistency of observations made by moderate resolution sensors commonly used for surface, atmospheric and cloud studies. Starting with TIROS-N in 1978, these sensors have provided a long time series of satellite data, which contain rich information pertaining to the state of many important environmental and meteorological variables. However, use of such diverse data sets requires a careful evaluation of their compatibility and consistency to avoid any artefacts. This study elaborates the influence of different SRFs on reflectance measurements in the visible and NIR channels and on the NDVI. The sensors examined included AVHRRs from NOAA-6 to the latest NOAA-16 as well as MODIS, VGT, GLI and a number of imagers on the geostationary satellites GOES –8-12, METEOSAT2-7, GMS-1-5. All the sensors were compared to the AVHRR/NOAA-9 radiometer, which was chosen as the reference.

The study illustrated that the differences in SRF are significant enough, that they need to be taken into account particularly for studies concerning inter-annual variations. The SRF effect is comparable in magnitude to the uncertainties caused by sensor calibration and the angular correction. Even among "the same type" instruments such as AVHRR, the effect of the varying spectral response function on surface and TOA spectral reflectances and NDVI vegetation index is sufficiently large to require correction. The observational results presented for MODIS and AVHRR NDVI are generally in good agreement with model simulations, both in sign and magnitude of the spectral response function effect.

ACKNOWLEDGEMENTS

REFERENCES

1. Berk A., and Co-Authors, "MODTRAN4 Version 2 User's manual". *Air Force Research Laboratory. Space Vehicles Directorate. Air Force Materiel Command*. Hanscom AFB, MA 01731-3010. 98pp, 2001.
2. Brest, C. L., W. B. Rossow, and M. D. Roiter, "Update on radiance calibrations for ISCCP", *J. Atmos. Oceanic. Technol.,* **14**, pp.1091-1109, 1997.
3. Cihlar, J., J. M. Chen, Z. Li, F. Huang, R. Latifovic, R. Dixon,"Can interannual land surface signal be discerned in composite AVHRR data?", *J. Geophys. Res.*, **103**, pp.23163-23172, 1998.

4. Cihlar, J., R. Latifovic, J. Chen, A. Trishchenko, Y. Du, G. Fedosejevs, and B. Guindon, "Systematic corrections of AVHRR image composites for temporal studies", *Remote Sens. Environ.* (in press), 2002.

5. Cihlar, J., I. Tcherednichenko, R. Latifovic, Z. Li, and J. Chen, "Impact of variable atmospheric water vapor content on AVHRR data corrections over land", *IEEE Trans. Geosci. Remote Sens.*, **39**, pp.173-180, 2000.

6. Csiszar, I., G. Gutman, P. Romanov, M. Leroy, O. Hautecoeur, "Using ADEOS/POLDER data to reduce angular variability of NOAA/AVHRR reflectances", *Remote Sens. Environ.*, **76**, 399-409, 2001.

7. Desormeaux, Y., W. B. Rossow, C. L. Brest, G. G. Campbell, " Nomalization and calibration of geostationary satellite radiances for the International Satellite Cloud Climatology Project", *J. Atmos. Ocean. Technol.* **10**, pp.304-325, 1993

8. Gobron, N., B. Pinty, M. M. Verstraete, and J-L. Widlowski, "Advanced vegetation indices optimized for up-coming sensors: Design, performance, and applications", *IEEE Trans. Geosci. Remote Sens.*, **38**, pp.2489-2505, 2000.

9. Gutman, G., A. Gruber, D. Tarpley, and R. Taylor, "Application of angular models to AVHRR data for determination of the clear-sky planetary albedo over land surfaces", *J. Geophys. Res.*, **94**, pp.9959-9970, 1989.

10. Gutman, G., "On the use of long-term global data of land reflectances and vegetation indices derived from the advanced very high resolution radiometer", *J. Geophys. Res.*, **104**, pp.6241-6255, 1999.

11. Gutman, G., I. Csiszar, P. Romanov, "Using NOAA/AVHRR products to monitor El Niño impacts: Focus on Indonesia in 1997-98", *Bull. Amer. Meteor. Soc.*, **81**, pp.1189-1205, 2000.

12. Kaufman, R.K., L. Zhou, Y. Knyazikhin, N. Shabanov, R. Myneni, and C. Tucker, "Effect of orbital drift and sensor changes on the time series of AVHRR vegetation index data", *IEEE Trans. Geosci. Remote Sens.,* **38**, pp.2584-2597, 2000.

13. Masonis, S. J., and S. G. Warren, "Gain of the AVHRR visible channel as tracked using bidirectional reflectance of Antarctic and Greenland snow", *Int. J. Remote Sens.,* **22**, pp.1495–1520, 2001.

14. Rao, C. R. N., and J. Chen, "Revised post-launch calibration of the visible and near-infrared channels of the Advanced Very High Resolution Radiometer (AVHRR) on the NOAA-14 spacecraft", *Int. J. Remote Sens.*, **20**, pp.3485-3491, 1999.

15. Rossow, W. B., and R. A. Schiffer, "Advances in understanding clouds from ISCCP", *Bull. Amer. Meteor. Soc.*, **80**, pp.2261-2287, 1999.

16. Rutan, D., and T. P. Charlock, "Spectral reflectance, directional reflectance, and broad-band albedo of the earth's surface", *Proc. 9th Conference on Atmospheric Radiation,* Long Beach, California, pp. 466-470, 1997.

17. Secker, J., K. Staenz, P. Budkewitsch, R. A. Neville, "A vicarious calibration of the Probe-1 hyperspectral sensor", *4th Int. Airborne Remote Sens. Conf. and Exhibition/21st Canadian Symp. on Remote Sens.,* Ottawa, Ontario, Canada, 21-24 June , pp.75-82, 1999.

18. Tahnk, W. R., and J. A. Coakley, "Updated calibration coefficients for NOAA-14 AVHRR channels 1 and 2", *Int. J. Re*mote Sens., **22**, pp.3053–3057, 2001.

19. Teillet, P. M., K. Staenz, and D. J. Williams, "Effects of spectral, spatial, and radiometric characteristics on remote sensing vegetation indices of forested regions", *Rem. Sens. Environ.*, **61**, pp.139-149, 1997.

20. Teillet, P. M., J. Barker, B. L. Markham, R. R. Irish, G. Fedosejevs, J. C. Storey, "Radiometric cross-calibration of the Landsat-7 ETM+ and Landsat-5 TM sensors based on tandem data sets", *Remote Sens. Environ.*, **78**, pp.39-54, 2001.

21. Trishchenko, A. P., Z. Li, F.-L. Chang, H. Barker, "Cloud Optical Depths and TOA Fluxes: Comparison Between Satellite and Surface Retrievals from Multiple Platforms", *Geophys. Res. Lett.*, **28**, pp.979-982, 2001.

22. Trishchenko, A. P., Z. Li, W. Park, J. Cihlar, "Corrections for the BRDF and topographic effects in satellite retrieval of surface spectral reflectance in solar spectral region", *In Proc. of the Int. Radiation Symp.IRS 2000.* St.Petersburg, Russia, August 2000. W.L. Smith and Y. Tymofeyev (eds). A. Deepak, v. **147**, pp.44-47, 2001.

23. Trishchenko, A.P., J. Cihlar, Z. Li, " Effect of spectral response function of surface reflectance and NDVI measured with moderate resolution satellite sensors", *Remote Sens. Environ.*, **81**, pp.1-18, 2002.

24. Vermote, E., D. Tanré, J. L. Deuzé, M. Herman, and J. J. Morcrette, "Second simulation of the satellite signal in the solar spectrum: An overview", *IEEE Trans. Geosci. Remote Sens.,* **35**, pp.675-686, 1997.

* trichtch@ccrs.nrcan.gc.ca; phone (613) 995 57 87; fax (613) 947 13 83; http://www.ccrs.nrcan.gc.ca, Canada Centre for Remote Sensing, Natural Resources Canada; 588 Booth Str., Ottawa, Ontario, Canada, K1A 0Y7.
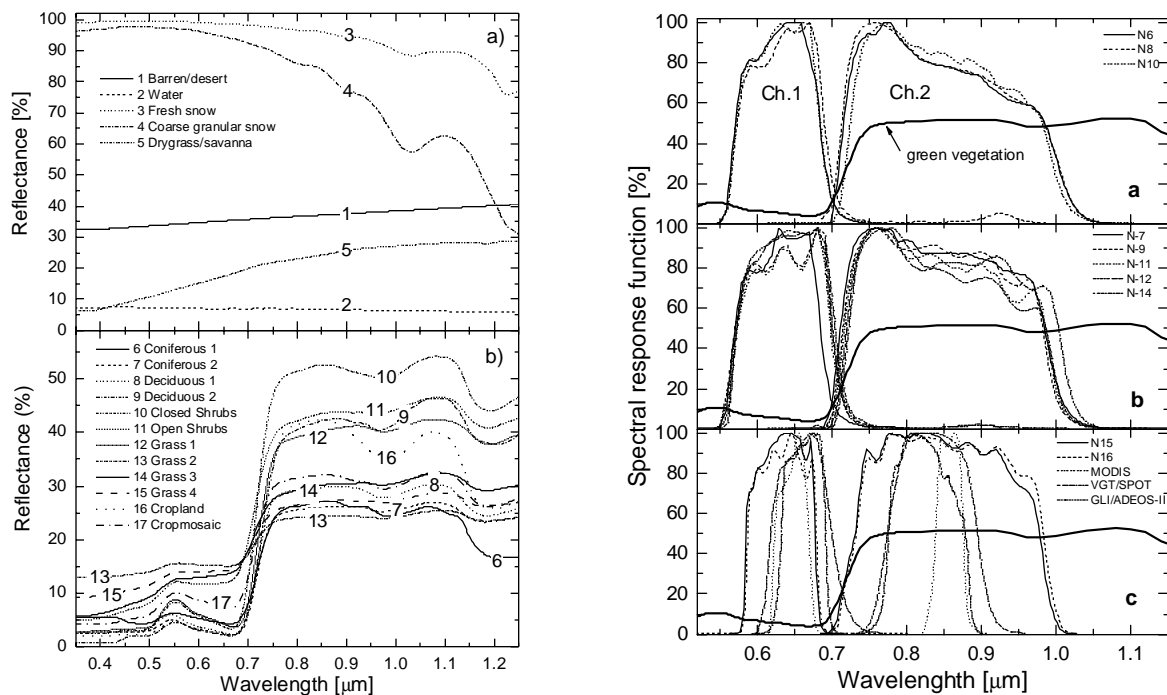
Figure 1. Spectral reflectance of some basic surface types (left) and spectral response functions of several sensors employed for land surface studies (right). Left panel: top – non-vegetated surfaces, bottom – various vegetation types. Right panel: top – AVHRR-1/NOAA-6, 8, 10 morning sensors; middle – AVHRR-2/NOAA-7, 9,11,12,14; bottom – AVHRR-3/NOAA-15, 16, MODIS (ch.1 and 2), VGT/SPOT and GLI/ADEOS-II.
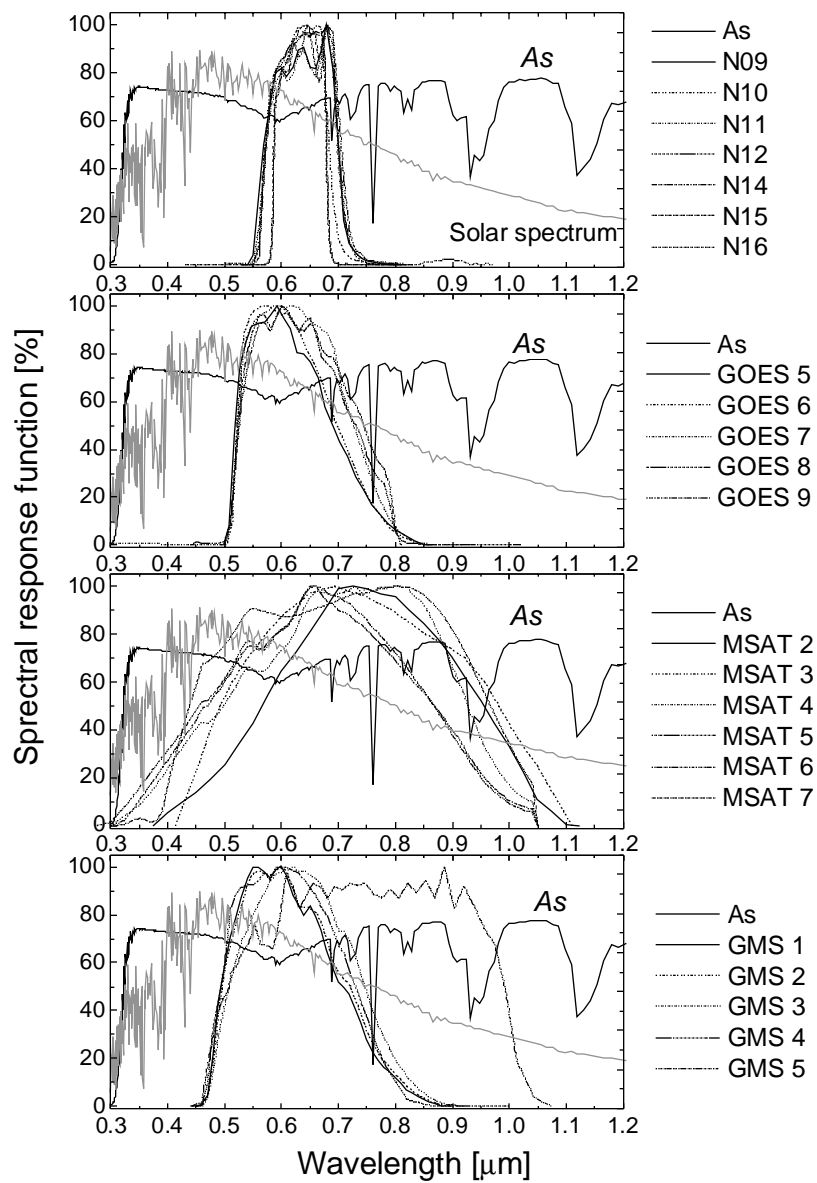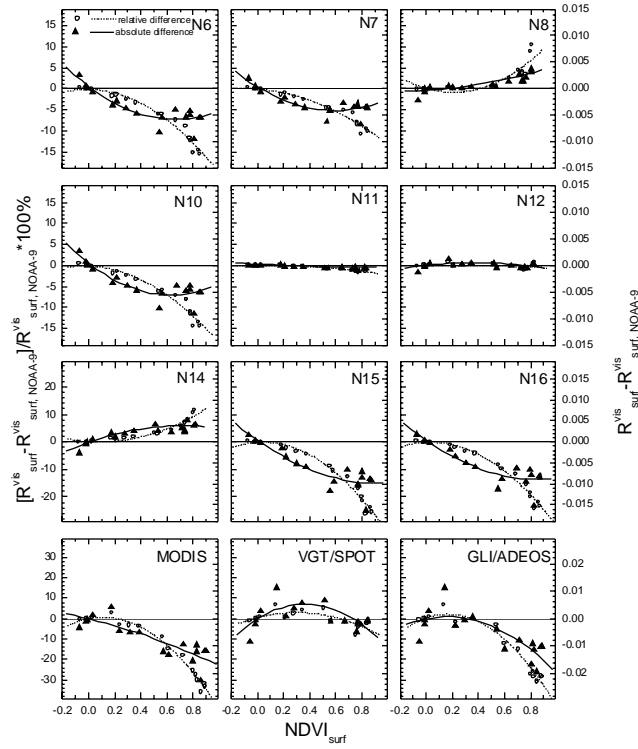
Figure 2. Spectral response functions of AVHRR/NOAA-9-16 and geostationary satellites GOES, METEOSAT, GMS. Spectral reflectance of *As* cloud with an optical depth of 20 and solar spectrum are plotted for reference.
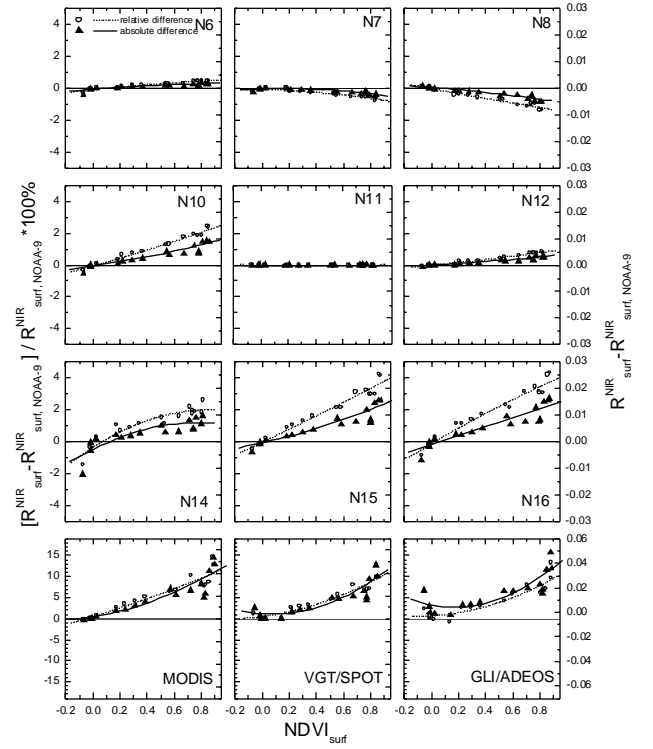
Figure 3. Difference in surface reflectance for visible (left) and NIR (right) channels with respect to corresponding channels of AVHRR/NOAA-9.
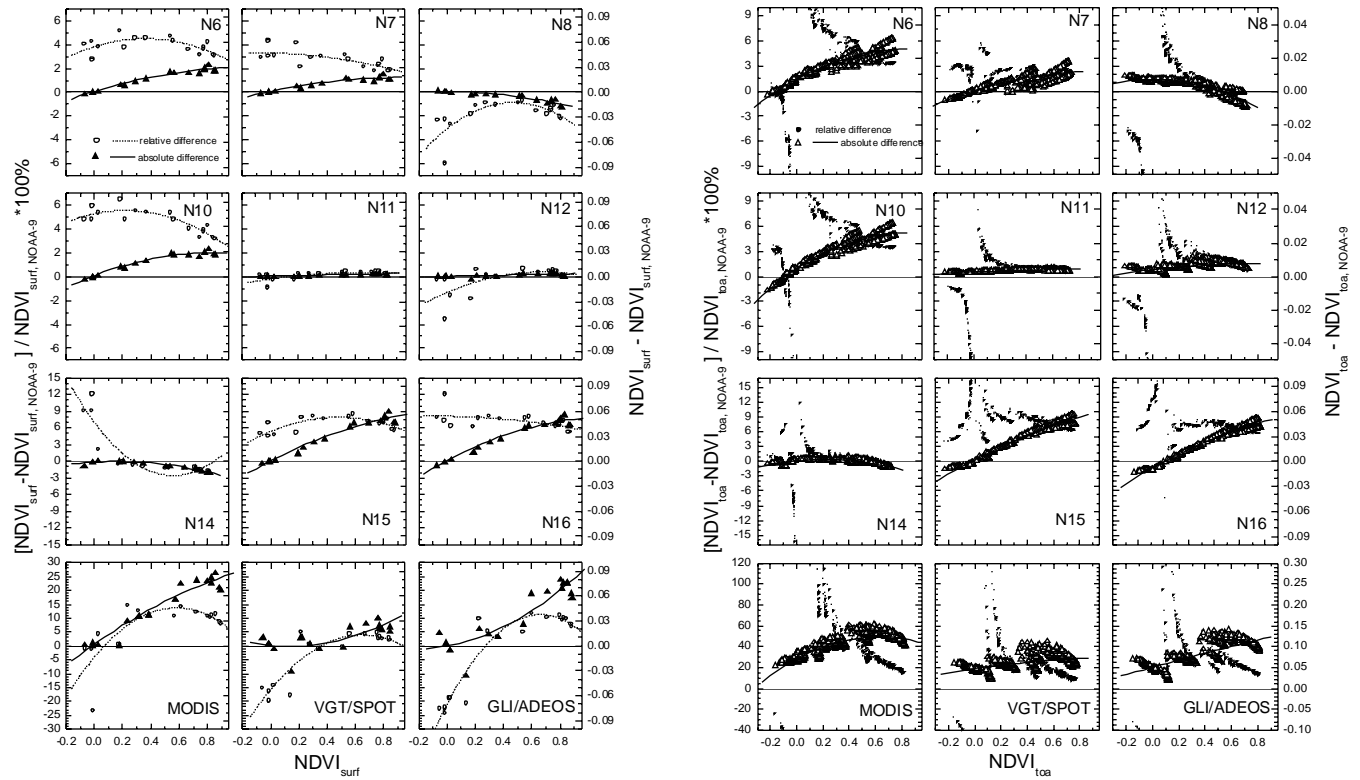
Figure 4. Difference in NDVI with respect to AVHRR/NOAA-9 at surface (left) and TOA (right) levels for various coarse resolution sensors.
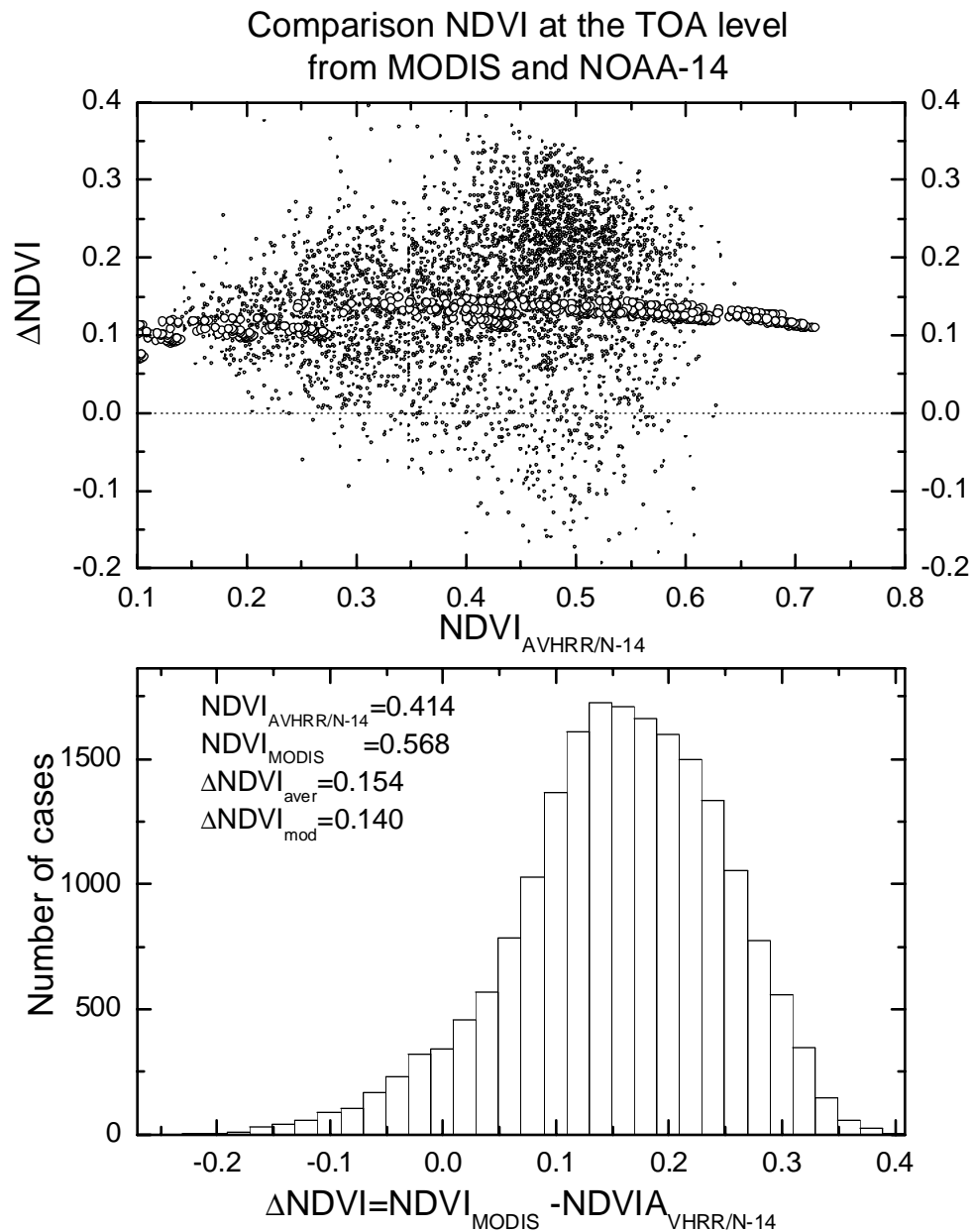
Comparison NDVI at the TOA level from MODIS and NOAA-14

$NDVI_{AVHRR/N-14}=0.414$
$NDVI_{MODIS}=0.568$
$\Delta NDVI_{aver}=0.154$
$\Delta NDVI_{mod}=0.140$

Figure 5. Modeled and observed differences in NDVI between AVHRR/NOAA-14 and MODIS. Comparison are for Southern Great Planes (SGP) area in Oklahoma for July, 2000.
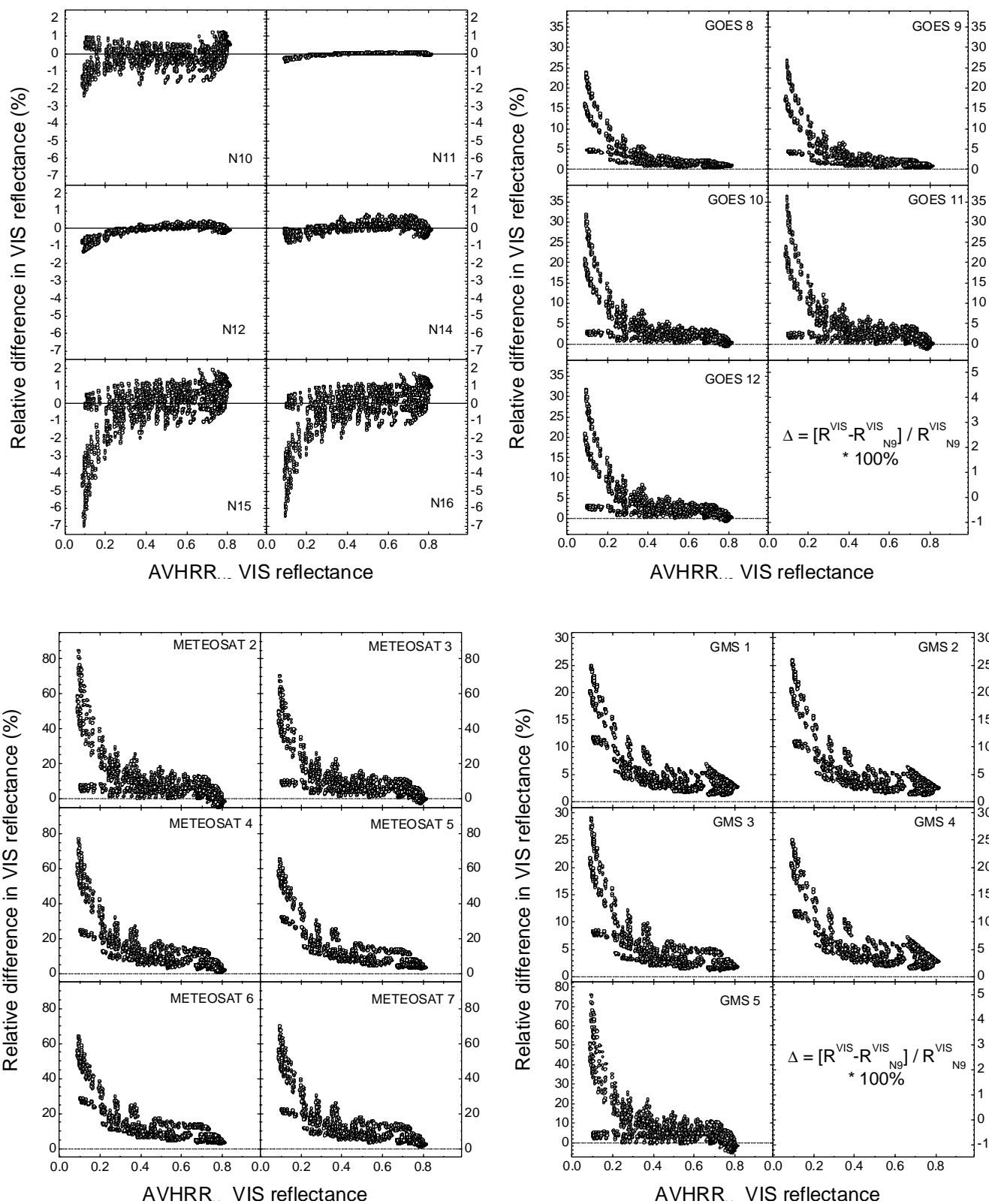
Figure 6. Relative differences in TOA reflectance for cloud scenes computed with respect to the AVHRR/NOAA-9 visible channel.